

See discussions, stats, and author profiles for this publication at: <https://www.researchgate.net/publication/262147466>

# Nanomolar Detection of Hypochlorite by a Rhodamine-Based Chiral Hydrazide in Absolute Aqueous Media: Application in Tap Water Analysis with Live-Cell Imaging

ARTICLE *in* ANALYTICAL CHEMISTRY · MAY 2014

Impact Factor: 5.64 · DOI: 10.1021/ac500418k · Source: PubMed

---

CITATIONS

16

---

READS

107

## 8 AUTHORS, INCLUDING:



[Abhishek Manna](#)

Indian Institute of Engineering Science and Te...

49 PUBLICATIONS 509 CITATIONS

[SEE PROFILE](#)



[Partha Saha](#)

Indian Agricultural Research Institute

27 PUBLICATIONS 221 CITATIONS

[SEE PROFILE](#)



[Ching Kheng Quah](#)

Universiti Sains Malaysia

245 PUBLICATIONS 844 CITATIONS

[SEE PROFILE](#)



[Hatem Abdel-Aziz](#)

National Research Center, Egypt

161 PUBLICATIONS 1,043 CITATIONS

[SEE PROFILE](#)

# Nanomolar Detection of Hypochlorite by a Rhodamine-Based Chiral Hydrazide in Absolute Aqueous Media: Application in Tap Water Analysis with Live-Cell Imaging

Shyamaprosad Goswami,<sup>\*,†,||</sup> Avijit Kumar Das,<sup>†</sup> Abhishek Manna,<sup>†</sup> Anup Kumar Maity,<sup>‡</sup> Partha Saha,<sup>‡</sup> Ching Kheng Quah,<sup>§</sup> Hoong-Kun Fun,<sup>§,||</sup> and Hatem A. Abdel-Aziz<sup>||,⊥</sup>

<sup>†</sup>Department of Chemistry, Indian Institute of Engineering Science and Technology (formerly Bengal Engineering and Science University), Shibpur, Howrah, West Bengal 711103, India

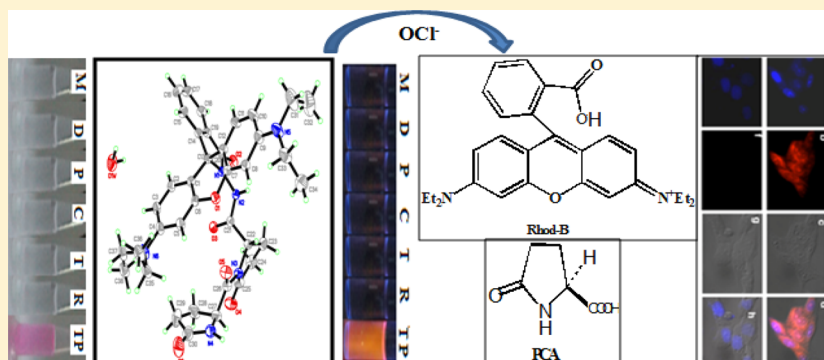
<sup>‡</sup>Crystallography and Molecular Biology Division, Saha Institute of Nuclear Physics, Kolkata, West Bengal 700064, India

<sup>§</sup>X-ray Crystallography Unit, School of Physics, Universiti Sains Malaysia, 11800 USM Penang, Malaysia

<sup>||</sup>Department of Pharmaceutical Chemistry, College of Pharmacy, King Saud University, Riyadh 11451, Saudi Arabia

<sup>⊥</sup>Department of Applied Organic Chemistry, National Research Centre, Dokki 12622, Egypt

## Supporting Information



**ABSTRACT:** By employing the oxidation property of hypochlorite ( $\text{OCl}^-$ ), a novel rhodamine-based hydrazide of the chiral acid ((S)-(-)-2-pyrrolidone-5-carboxylic acid) (RHHP) was designed and synthesized for detection of  $\text{OCl}^-$  absolutely in aqueous medium at nanomolar level. The structure of the chiral sensor was also proved by the X-ray crystallography. The bioactivity and the application of the probe for detection of  $\text{OCl}^-$  in natural water system have been demonstrated. A plausible mechanism for oxidation of the sensor followed by hydrolysis is also proposed. The sensibility of the receptor toward  $\text{OCl}^-$  was studied in absolute aqueous media, and the detection limit of hypochlorite-mediated oxidation to the receptor in nanomolar level makes this platform (RHHP) an ultrasensitive and unique system for  $\text{OCl}^-$  oxidation.

Hypochlorite anion ( $\text{OCl}^-$ ) is broadly engaged in our daily life, such as in household bleach, cooling water treatment, disinfection of drinking water, and cyanide treatment with the concentration of millimolar to micromolar range. Among the most reactive oxygen (ROS) and reactive nitrogen species (RNS),<sup>1,2</sup> hypochlorite anion ( $\text{OCl}^-$ ) and its protonated form hypochlorous acid (HOCl) are the geographically most important reactive oxygen species (ROS).<sup>3</sup> In the physiological pH windows, HOCl (weakly acidic) is partially dissociated into  $\text{OCl}^-$ . Myeloperoxidase (MPO) is a heme-containing enzyme, and from the reaction of  $\text{H}_2\text{O}_2$  and chloride ion catalyzed by heme enzyme, hypochlorite is generated in organisms.<sup>4</sup> The damage of tissue including diseases, such as atherosclerosis, arthritis, and cancers, is probably due to the critical involvement of  $\text{OCl}^-$ .<sup>5,6</sup> For the effective control and recovery of the drinking water quality, the understanding of microbial ecology in the drinking water distribution system,<sup>7</sup> pathogenic bacterial

growth,<sup>8</sup> microbial population dynamics,<sup>9</sup> and community structures<sup>10</sup> is not only crucial but it is also essential to detect and monitor  $\text{OCl}^-$  residues in tap water monitoring and also their accumulation in living organisms. Therefore, it is essential to develop efficient probes for  $\text{OCl}^-$  detection. The most reported selective and sensitive fluorescent oxidizable moieties by different oxidants bearing oxidizable auxochromic groups are *p*-methoxyphenol, thiol,<sup>11</sup> dibenzoylhydrazine,<sup>12</sup> hydroxamic acid,<sup>13</sup> oxime derivatives,<sup>14</sup> oxazine-conjugated nanoparticle probe,<sup>15</sup> and different metal complexes.<sup>16</sup> Long et al.<sup>17</sup> recently reported a hydrazide moiety containing dual fluorophores for  $\text{OCl}^-$  detection in micromolar level in mixed aqueous media

Received: January 29, 2014

Accepted: May 8, 2014

Published: May 8, 2014



Scheme 1. Schematic Representation for Synthesis of RHHP

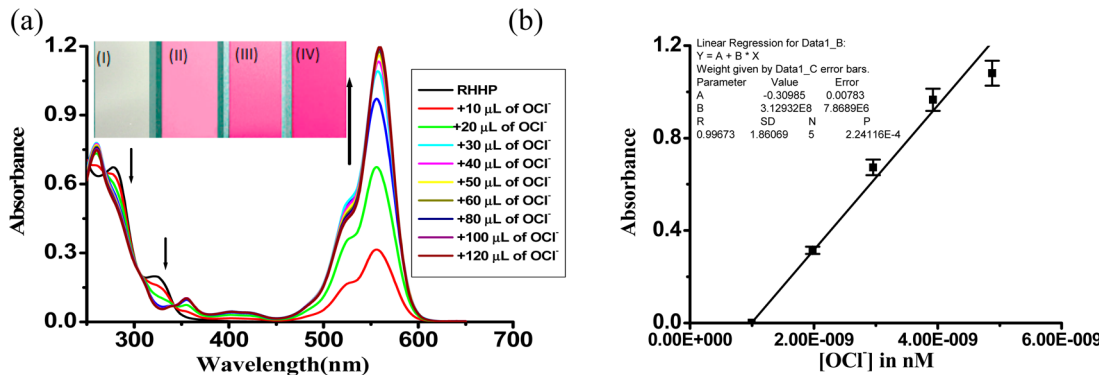
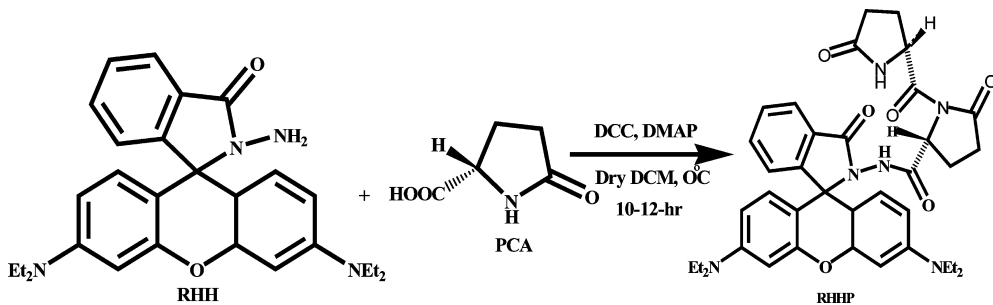


**Figure 1.** (a) UV-vis spectra of RHHP ( $c = 1.0 \times 10^{-7}$  M) in aqueous HEPES buffer solution upon addition with stock solution of OCl<sup>-</sup> ( $c = 2 \times 10^{-7}$  M) at pH 7.4. Left inset: visualized color changes in test strips of RHHP in the solid phase with different concentrations of OCl<sup>-</sup>: (I) RHHP itself and gradual addition of OCl<sup>-</sup> at (II)  $c = 1.0 \times 10^{-6}$  M, (III)  $c = 1 \times 10^{-5}$  M, and (IV)  $c = 1 \times 10^{-4}$  M concentration. (b) Binding isotherms were recorded at 555 nm with the change of the concentration of OCl<sup>-</sup> (nanomolar range) and the linear detection range including the error bars.

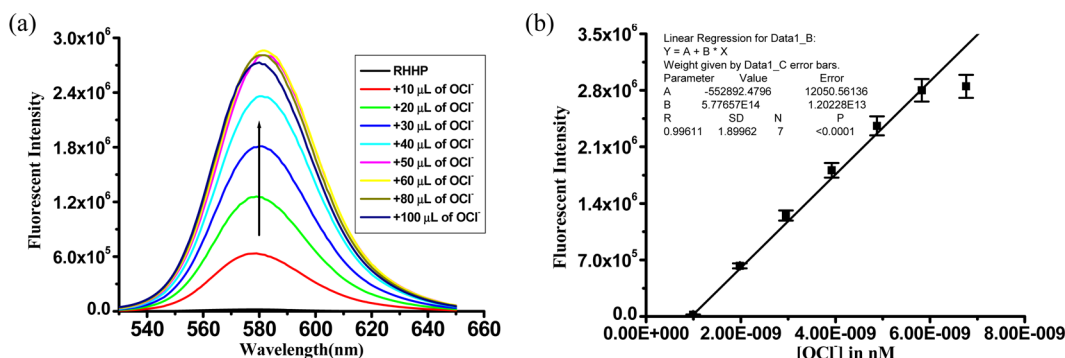


**Figure 2.** (a) Fluorescence spectra of the receptor RHHP ( $c = 1 \times 10^{-7}$  M) with stock solution of OCl<sup>-</sup> ( $c = 2 \times 10^{-7}$  M) in aqueous HEPES buffer solution at pH 7.4. (b) Binding isotherms were recorded at 580 nm with the change of concentration of OCl<sup>-</sup> and the linear detection range including the error bars.

without bioimaging, but here our designed chiral receptor (S)-(-)-2-pyrrolidone-5-carboxylic acid (RHHP) detects OCl<sup>-</sup> in completely aqueous media in nanomolar level with bioimaging. In our case, also hypochlorite-mediated oxidation of RHHP followed by hydrolysis at different proportions of water giving different intensities of color and fluorescence has been well-demonstrated. By taking all these properties into account, herein, we report the design, synthesis, and X-ray structure of a chiral hydrazide (RHHP) having rhod-B of high fluorescence quantum yield and large absorption coefficient<sup>18</sup> based on “off-on” colorimetric and fluorimetric response toward hypochlorite. The synthesis of the RHHP is delineated in the following scheme (Scheme 1).

The intermediate hydrazone (RHH) derivative of rhod-B dye is prepared according to the reported literature.<sup>19</sup> The target

chemosensor was prepared by the DCC coupling reaction of rhod-B hydrazone (RHH) with the chiral acid (S)-(-)-2-pyrrolidone-5-carboxylic acid (PCA) (Scheme 1). Interestingly, by these two coupling reactions, there is formation of one hydrazide between the rhodamine hydrazone dye with the chiral acid (PCA) and the other amide link by the coupling reaction among this hydrazide with the other PCA resulting in the desired sensor with a highly reactive and sensitive chiral zone which is highly oxidizable by hypochlorite in absolute aqueous media over other oxidants. This OCl<sup>-</sup> sensing by RHHP shows high suitability for tap water monitoring and in vivo studies. The high selectivity and sensitivity of RHHP for OCl<sup>-</sup> detection were achieved probably by introducing highly reactive and easily hydrolyzable triketo functionality along with highly reactive and acidic —NH links which favor the

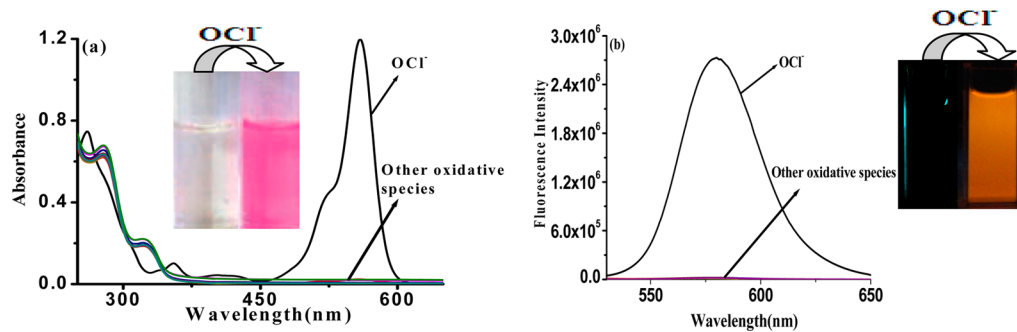


**Figure 3.** (a) UV–vis absorption spectra of RHHP ( $c = 1 \times 10^{-7}$  M) in aqueous HEPES buffer solution at pH 7.4 upon titration with 2.0 equiv of each of the different guest oxidative species ( $c = 2 \times 10^{-7}$  M in stock solution). (b) Fluorescence spectra of RHHP ( $c = 1 \times 10^{-7}$  M) in aqueous HEPES buffer upon titration with 3.0 equiv of each of the different guest oxidative species ( $c = 2 \times 10^{-7}$  M in stock solution).

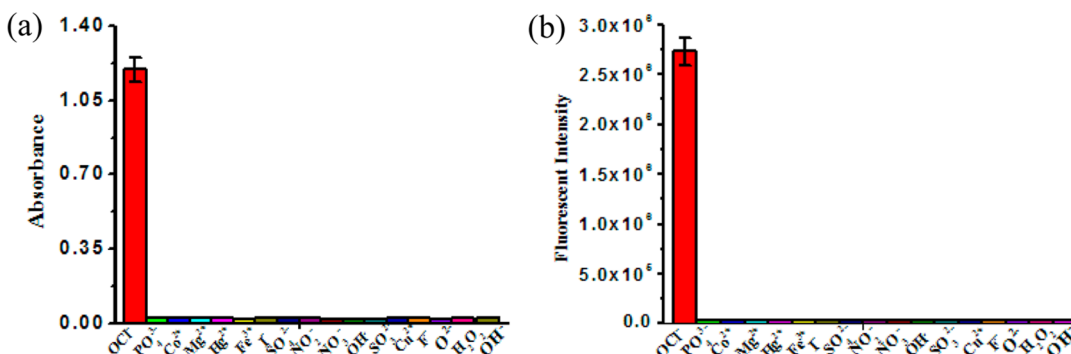


**Figure 4.** Selectivity profile diagram in bar representation including error bars (error amount, 5%; Y error bar for both [ $\pm$ ] deviation). Changes of (a) absorbance and (b) fluorescence of RHHP ( $c = 1 \times 10^{-7}$  M) in aqueous HEPES buffer solution at pH 7.4 upon addition of the different guest oxidative species ( $c = 2 \times 10^{-7}$  M in stock solution): red bars (RHHP +  $\text{OCl}^-$ ) and other bars for different oxidative species.

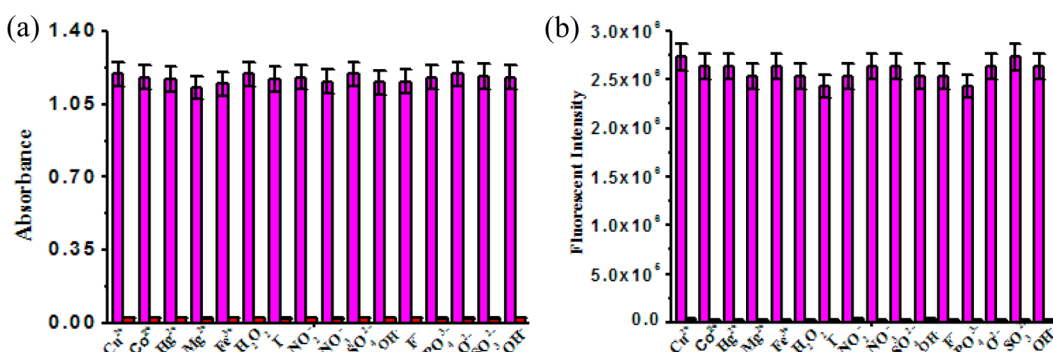


**Figure 5.** Hypochlorite selectivity profile of the sensor RHHP in bar representation including error bars (error amount, 5%; Y error bar for both [ $\pm$ ] deviation): (red bars) change of (a) absorbance and (b) emission intensity of RHHP ( $c = 1 \times 10^{-7}$  M) + 2.0 equiv of different oxidative species ( $c = 2 \times 10^{-7}$  M in stock solution); (violet bars) change of (a) absorbance and (b) emission intensity of sensor + 2.0 equiv of different anions, followed by 2.0 equiv of  $\text{OCl}^-$ .

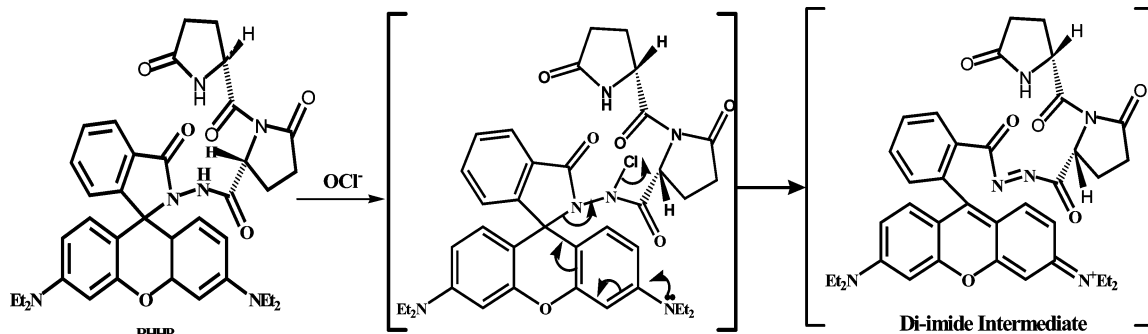
hypochlorite oxidation in absolute water media. The different optical properties, i.e., absorption and fluorescence response of RHHP ( $c = 1 \times 10^{-7}$  M), toward different oxidants and anions such as  $\text{Cu}^{2+}$ ,  $\text{Co}^{2+}$ ,  $\text{Hg}^{2+}$ ,  $\text{Mg}^{2+}$ ,  $\text{Fe}^{3+}$ ,  $\text{F}^-$ ,  $\text{I}^-$ ,  $\text{NO}_2^-$ ,  $\text{NO}_3^-$ ,  $\text{SO}_4^{2-}$ ,  $\text{SO}_3^{2-}$ ,  $\text{PO}_4^{3-}$ ,  $\text{OH}^-$ ,  $\text{H}_2\text{O}_2$ ,  $\text{O}^{2-}$ ,  $\text{OH}^\bullet$  ( $c = 2 \times 10^{-7}$  M) were studied in absolute aqueous HEPES buffer solution at pH 7.4. In absorption spectra, RHHP exhibits two absorption bands at 278 and 325 nm. Upon addition of increasing concentrations of  $\text{OCl}^-$ , typical absorption at 555 nm enhanced significantly followed by increase in a small band at 260 nm with two isosbestic points at 270 and 340 nm (Figure 1).

The absorption band at 555 nm is increased by 397-fold. To investigate the handy application of sensor RHHP, test strips were prepared by immersing the thin-layer chromatography

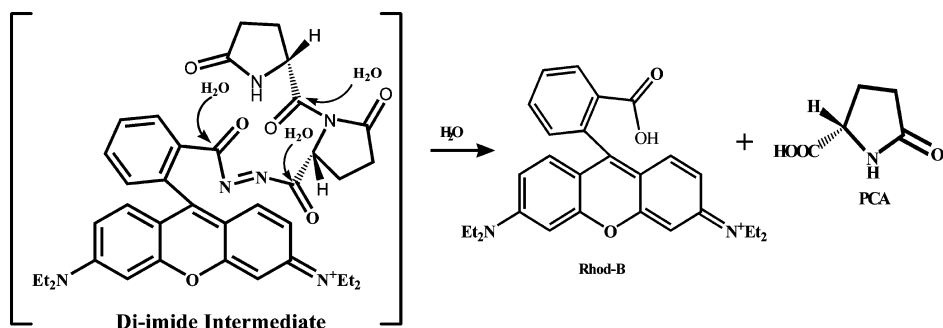
(TLC) plates into the receptor solution ( $c = 1 \times 10^{-7}$  M) at pH 7.4. The test strips containing RHHP were utilized to sense  $\text{OCl}^-$  at different conditions. As shown in the left inset of Figure 1, with increase of concentration of  $\text{OCl}^-$  to the receptor solution, the visualized pink color in the solid phase (test strips) is growing to be more intense. This type of dipstick method is very much helpful for the instant qualitative information without remedying any type of time-consuming instrumental analysis.

In the fluorescence response of RHHP, there was no typical fluorescence observable in absence of  $\text{OCl}^-$  to the receptor solution due to its consistency of the spirolactam structure of the rhodamine fluorophore in RHHP.

Scheme 2. Schematic Pathway of Hypochlorite-Mediated Oxidation of RHHP to Form the Diimide Intermediate



Scheme 3. Hydrolytic Behavior of the Diimide Intermediate



But hypochlorite-mediated oxidation significantly opens the spirolactam moiety and results in the formation of reddish-yellow fluorescence in the emission spectra with increasing concentrations of OCl<sup>-</sup>.

The result is the appearance of pink color followed by the increase of 139-fold emission intensity at 580 nm (Figure 2) and 55-fold ( $\Phi/\Phi_0 = 0.273/0.005 = 55$ ,  $\lambda_{\text{max}}(\text{em}) = 520$  nm) fluorescence quantum yield on excitation at 520 nm. The addition of other interfering oxidants is almost neutral toward the oxidation of the hydrazide moiety of RHHP (Figure 3).

The neutral behavior of the other oxidative species except OCl<sup>-</sup> is also shown by the bar diagram. As shown in Figure 4, the addition of OCl<sup>-</sup> in RHHP solution the oxidative cleavage increases the absorbance and fluorescence color of the resulting solution significantly, which is shown by the red bar.

To further explore the selectivity of RHHP toward OCl<sup>-</sup>, the competition experiment was carried out using receptor solution in the presence of hypochlorite mixed with the other oxidative species.

The enhancement of absorbance and fluorescence by hypochlorite-mediated oxidation of RHHP almost remains unperturbed in the presence of other oxidative species, and they also become innocent toward sensing to the receptor as well as the oxidative cleavage of the sensor (Figure 5). For hypochlorite, oxidation of the rhodamine derivative is very much pH-dependent. To obtain the optimum conditions for using RHHP as a unique hypochlorite sensor, pH titration was carried out (Supporting Information Figure S2). The pH titration experiment revealed that RHHP does not show any significant coloration within the pH range from 6 to 12.5, which indicates that the molecule exists in the spirocyclic form in this definite pH range. In strong acidic conditions (pH < 5), protonation to rhodamine moiety causes the red coloration along with strong reddish-yellow fluorescence due to opening of the spirolactam ring. Therefore, for the optimum usage of

RHHP as a hypochlorite sensor by oxidative pathway, the pH of the medium should be maintained within near-neutral pH range (pH 7.4). It is revealed that minimum 2.9 nM of OCl<sup>-</sup> can be detected by RHHP solution ( $c = 1 \times 10^{-7}$  M) in UV-vis titration. In the fluorescence titration experiments, the detection limit of OCl<sup>-</sup> toward RHHP is determined to be 1.4 nM using the equation  $\text{DL} = (K)(S_b/S)$ , where  $K = 3$ ,  $S_b$  is the standard deviation of the blank solution, and  $S$  is the slope of the calibration curve (Figure S1, Supporting Information).

The appearance of absorption and emission color of RHHP on OCl<sup>-</sup> addition is due to spirolactam ring opening of the rhodamine moiety. However, the pathway of ring opening is different for different analytes. For the majority of cations, the ring opening occurs via the chelation of cations with the rhodamine-linked derivative resulting in the formation of a chelation-enhanced (CHEF) “off-on” colorimetric and fluorescence probe for different metal ions based on the conversion of spirolactam (colorless, nonfluorescent) to ring-open amide (pink colored, strong fluorescence) equilibrium of the rhodamine dye.<sup>20</sup>

Metal ion coordination followed by the ring opening of the rhodamine moiety does not lead to the loss of any group of the binding zone. But, here the hydrazide moiety of RHHP was oxidized by OCl<sup>-</sup> to form a diimide intermediate (Scheme 2), which underwent further hydrolysis (Scheme 3) to produce strongly reddish-yellow fluorescence and pink-colored rhod-B along with the parent chiral acid PCA.

The rate of hydrolysis of the diimide intermediate is very much solvent-dependent. As water is highly responsible for the hydrolysis of diimide intermediate, in pure acetonitrile, the RHHP does not give any significant color in the presence of OCl<sup>-</sup>. With increase in proportion of water in acetonitrile, the hydrolysis rate of the diimide intermediate significantly intensifies, yielding more intense pink color and reddish-yellow fluorescence, which is shown in Figure 6.

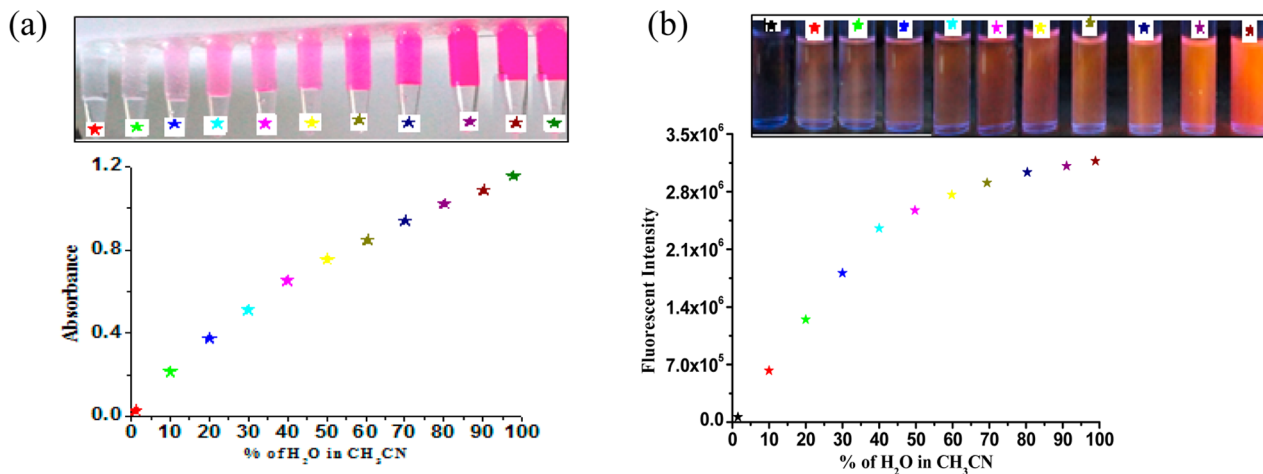


**Figure 6.** Intensity of (a) absorption and (b) fluorescent color appearance with the addition of different proportions of H<sub>2</sub>O (10%, 20%, 30%, 40%, 50%, 60%, 70%, 80%, 90%, 100%) in CH<sub>3</sub>CN containing RHHP ( $c = 1 \times 10^{-7}$  M) with 1.0 equiv of OCl<sup>-</sup> ( $c = 2 \times 10^{-7}$  M in stock solution) at pH 7.4. Each starmark indicates the color intensity to the various proportions of H<sub>2</sub>O.

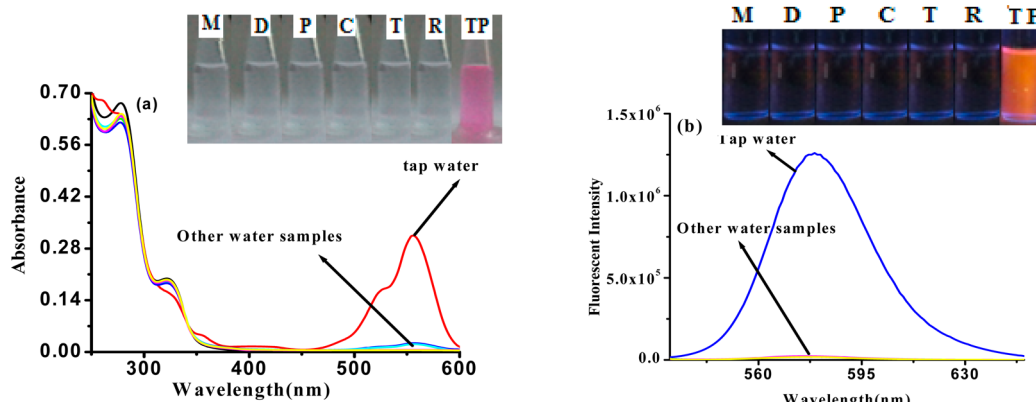


**Figure 7.** Photophysical sensibility of RHHP (10  $\mu$ M) to the different water samples in HEPES buffer at pH 7.4. (a) The changes of absorption of RHHP with differently analyzed water samples. (b) Changes of emission intensity of RHHP with differently analyzed water samples. Inset: the respective naked eye color and fluorescence changes for different water samples.

The rate of hydrolysis and the cleavage of the hypochlorite-mediated hydrazide linkage is very much fast (<30 s; saturation occurs at about 200 s in absorption as well as 120 s in emission spectra) to free the rhod-B and the chiral acid. From the changes of these optical properties at different time intervals and using the first-order rate equation, the rate of hypochlorite-mediated oxidation of RHHP can be calculated. The rate constants that we obtained from the time versus absorbance plot (at fixed wavelength at 555 nm, Supporting Information Figure S3) and time versus fluorescent intensity plot (at fixed wavelength at 580 nm, Supporting Information Figure S4) are  $4.07 \times 10^{-2}$  and  $3.47 \times 10^{-2} \text{ s}^{-1}$ , respectively. As OCl<sup>-</sup> has high oxidizing property, the hydrolysis of hypochlorite-mediated oxidized diimide intermediate followed by the cleavage of the amide linkage between the two PCA releases the rhod-B fluorophore and PCA. To confirm this hypothesis, the RHHP was treated with OCl<sup>-</sup> and the products were isolated and characterized by high-resolution mass spectrometry (HRMS) and <sup>1</sup>H NMR analysis. The respective peaks at  $m/z = 444.1886$  for [rhod-B + H]<sup>+</sup> (Supporting Information Figure 11) and 130.0492 for (PCA + H)<sup>+</sup> (Supporting Information Figure 13) confirm the identity of products.

As our rhodamine-based system RHHP acts as an ultra-sensitive and nanomolar-detectable probe for OCl<sup>-</sup> in absolute

aqueous media, it can be used for analyzing natural water system, i.e., to differentiate different types of water samples (Figure 7). The experiment was done by Millipore deionized water (M), distilled water (D), pond water (P), canal water (C), tubewell water (T), rainwater (R), and tap water (TP). These selected water samples were analyzed by using RHHP without and with addition of OCl<sup>-</sup>. Without addition of OCl<sup>-</sup>, no significant color was observed in other water samples even in higher concentration (600  $\mu$ L) except tap water.

The addition of OCl<sup>-</sup> resulted in a remarkable color appearance in each case (Supporting Information Figure S6). Nevertheless, in the case of drinking water from taps, 50  $\mu$ L of tap water led to an increase of the “naked eye” pink color and reddish-yellow fluorescence intensity of the sensing system and these colors increased evenly with the increase of amount of tap water, which further revealed that such an ultrasensitive sensing system, RHHP, was sensitive toward OCl<sup>-</sup> even in real water samples with significantly more complex compositions rather than the laboratory environments (Supporting Information Figure S5). The concentration of OCl<sup>-</sup> in tap water was quantified to be 0.04  $\mu$ M comparing with the UV-vis titration data.

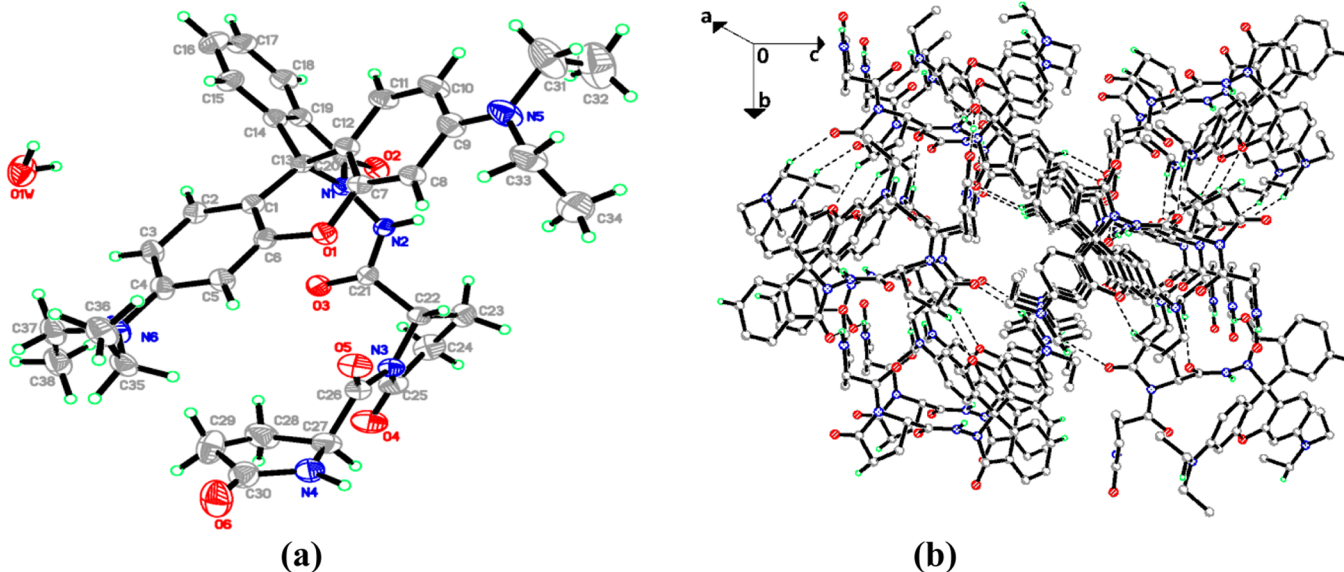


**Figure 8.** (a) Structure of receptor RHHP, showing displacement ellipsoids drawn at the 50% probability level. Hydrogen atoms are drawn as circles with small radii. (b) The molecules are linked to form a three-dimensional network. H atoms not involved in intermolecular interactions (dashed lines) have been omitted for clarity.

## X-RAY CRYSTALLOGRAPHY

The three-dimensional structure of receptor RHHP was confirmed by single-crystal X-ray diffraction studies (Figure 8a). The asymmetric unit of structure consists of a receptor RHHP and a water molecule. The least-squares plane (rms deviation of 0.245 Å) of the 9H-xanthene ring system forms dihedral angles of 85.26(10)°, 56.82(16)°, and 46.32(19)° with the isoindoline ring system (rms deviation of 0.016 Å) and the least-squares planes of the two pyrrolidine rings [N3/C22–C25 (rms deviation of 0.229 Å) and N4/C27–C30 C25 (rms deviation of 0.109 Å)], respectively.

The dihedral angle between the least-squares planes of the two pyrrolidine rings is 65.5(2)°. The pyrrolidine rings adopt twisted (atoms C22–C23) and envelope conformations (atom C28). In the crystal (Figure 8b), molecules are linked via intermolecular N–H···O and C–H···O bifurcated acceptor bonds (Supporting Information Table S1), together with other N–H···O, O–H···O, and C–H···O hydrogen bonds (Supporting Information Table S2), forming a three-dimensional network.

## CELL IMAGING

To investigate the membrane permeability of the RHHP and its oxidation by  $\text{OCl}^-$  ion in a living system, HeLa cells were first developed. Then the cells were treated with  $\text{OCl}^-$  followed by the addition of RHHP. An intense red fluorescence was observed in the cytoplasm of the cells when cells were treated with  $\text{OCl}^-$  followed by the RHHP, but in control experiment no red fluorescence was observed from the cells when they were treated only with RHHP in the same channel (Figure 9). When DAPI was treated with the cells, expected strong blue fluorescence could be obtained only from the nucleus. Possibly by oxidative pathway the cell membranes get incorporated with  $\text{OCl}^-$  to carry forward to the cytoplasm in the presence of the receptor to make it fluorescence-responsive (red) by oxidation of the receptor, and this result clearly establishes that the oxidized probe accumulates in the endo- and exomembranes including the nuclear membrane giving red fluorescence.

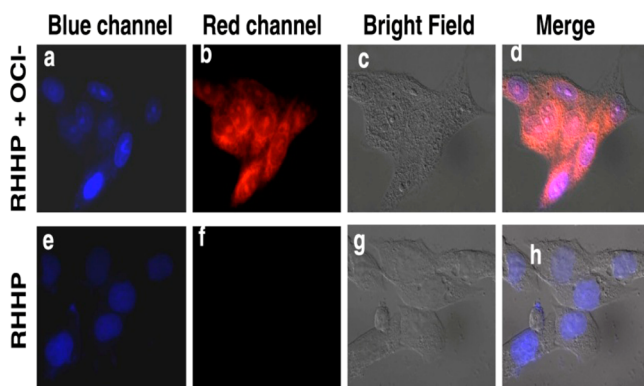


**Figure 9.** Fluorescence images of HeLa cells incubated with 50  $\mu\text{M}$  of the RHHP in presence (a and b) and in absence (e and f) of 50  $\mu\text{M}$  of  $\text{OCl}^-$ . Corresponding bright-field images (c and g) and merged images (d and h) of the cells.

## CONCLUSIONS

Thus, we have developed a highly reactive and specific chiral rhodamine-based chemosensor for the detection of  $\text{OCl}^-$  by an oxidative pathway. Interestingly, here we see that the increase in the keto functionality and the amide linkage creates a highly reactive indicator site to RHHP for  $\text{OCl}^-$  oxidation at nanomolar level in absolute aqueous media. The mechanism for hypochlorite-mediated oxidation of RHHP followed by hydrolysis is also well-recommended. The probe was successfully applied for the detection of  $\text{OCl}^-$  in tap water and for staining bioactivity.

## EXPERIMENTAL SECTION

**General.** Unless otherwise mentioned, chemicals and solvents were purchased from Sigma-Aldrich Chemicals Private Limited and were used without further purification. Melting points were determined on a hot-plate melting point apparatus in an open-mouth capillary and are uncorrected.  $^1\text{H}$  NMR and  $^{13}\text{C}$  NMR spectra were recorded on a Bruker 300 MHz instrument. For NMR spectra,  $\text{CDCl}_3$  and  $\text{MeOD}$  were used as

solvent using TMS as an internal standard. Chemical shifts are expressed in  $\delta$  units, and  $^1\text{H}$ - $^1\text{H}$  coupling constants in Hz. UV-vis titration experiments were performed on a JASCO UV-V530 spectrophotometer, and the fluorescence experiment was done using a PerkinElmer LS 55 fluorescence spectrophotometer using a fluorescence cell of 10 mm path. Single-crystal X-ray analysis was performed on a Bruker APEX II Duo CCD area-detector diffractometer using Mo  $\text{K}\alpha$  radiation ( $\lambda = 0.71073 \text{ \AA}$ ). The pH titration was carried out by using an Agilent 8453 pH meter.

**General Method of UV-Vis and Fluorescence Titration.** **UV-Vis Method.** For UV-vis and fluorescence titrations, a stock solution of the sensor was prepared ( $c = 1 \times 10^{-7} \text{ M}$ ) in absolute aqueous HEPES buffer solution at pH 7.4. The solutions of the various oxidants and anions like  $\text{Cu}^{2+}$ ,  $\text{Co}^{2+}$ ,  $\text{Hg}^{2+}$ ,  $\text{Mg}^{2+}$ ,  $\text{Fe}^{3+}$  (as their chloride salts),  $\text{F}^-$ ,  $\text{I}^-$ ,  $\text{NO}_2^-$ ,  $\text{NO}_3^-$ ,  $\text{SO}_4^{2-}$ ,  $\text{SO}_3^{2-}$ ,  $\text{PO}_4^{3-}$ ,  $\text{OH}^-$  (as their tetrabutylammonium salts),  $\text{H}_2\text{O}_2$ ,  $\text{O}^{2-}$ , and  $\text{OH}^\bullet$  (From Fenton's reagent) in the order of  $2 \times 10^{-7} \text{ M}$  were also prepared as a stock solution. Stock solutions of the sensor ( $c = 1 \times 10^{-7} \text{ M}$ ) and different oxidants ( $c = 2 \times 10^{-7} \text{ M}$ ) were prepared separately. With increase in concentration of the stock solution of the different oxidants ( $c = 2 \times 10^{-7} \text{ M}$ ) to the receptor solution ( $2 \text{ mL} \approx 2000 \mu\text{L}$ ), the UV-vis titration has been carried out.

**Fluorescence Method.** For fluorescence titrations, a stock solution of the sensor ( $c = 1 \times 10^{-7} \text{ M}$ ) was prepared in absolute aqueous HEPES buffer solution at pH 7.4. The solutions of the various oxidants and anions like  $\text{Cu}^{2+}$ ,  $\text{Co}^{2+}$ ,  $\text{Hg}^{2+}$ ,  $\text{Mg}^{2+}$ ,  $\text{Fe}^{3+}$  (as their chloride salts),  $\text{F}^-$ ,  $\text{I}^-$ ,  $\text{NO}_2^-$ ,  $\text{NO}_3^-$ ,  $\text{SO}_4^{2-}$ ,  $\text{SO}_3^{2-}$ ,  $\text{PO}_4^{3-}$ ,  $\text{OH}^-$  (as their tetrabutylammonium salts),  $\text{H}_2\text{O}_2$ ,  $\text{O}^{2-}$ , and  $\text{OH}^\bullet$  (from Fenton's reagent) in the order of  $2 \times 10^{-7} \text{ M}$  were also prepared as a stock solution. Stock solutions of the sensor ( $c = 1 \times 10^{-7} \text{ M}$ ) and different oxidants ( $c = 2 \times 10^{-7} \text{ M}$ ) were prepared separately. With increase in concentration of the stock solution of the different oxidants ( $c = 2 \times 10^{-7} \text{ M}$ ) to the receptor solution ( $2 \text{ mL} \approx 2000 \mu\text{L}$ ), the fluorescence titration has been carried out.

**Cell Culture and Fluorescence Microscopy.** HeLa cells were grown in Dulbecco's modified Eagle's medium (DMEM) supplemented with 10% fetal bovine serum and penicillin-streptomycin (0.5 U/mL of penicillin and 0.5  $\mu\text{g}/\text{mL}$  streptomycin) on a coverslip in 35 mm dishes at 37 °C in an atmosphere of air with 5%  $\text{CO}_2$  and constant humidity. The cells were initially incubated with the addition of 50  $\mu\text{M}$  of  $\text{OCl}^-$  in the growth medium for 45 min. After washing three times with phosphate-buffered saline (PBS), fresh growth medium containing 50  $\mu\text{M}$  of RHHP was added and the cells were further incubated for 45 min. Following the incubation, the cells were washed three times with PBS and the imaging was carried out using Zeiss Axio Observer fluorescence microscope equipped with an Apotome apparatus.

**Determination of Fluorescence Quantum Yield.** Here, the quantum yield  $\varphi$  was measured by using the following equation:

$$\varphi_x = \varphi_s (F_x/F_s)(A_s/A_x)(n_x^2/n_s^2)$$

where X and S indicate the unknown and standard solution, respectively,  $\varphi$  = quantum yield,  $F$  = area under the emission curve,  $A$  = absorbance at the excitation wavelength, and  $n$  = index of refraction of the solvent. Here  $\varphi$  measurements were performed using rhodamine-6G in ethanol, as standard [ $\Phi = 0.95$ ] (error ~10%).

## Methods for the Preparation of the Receptor.

**Synthesis of RHHP.** (*S*)-(–)-2-Pyrrolidone-5-carboxylic acid (250 mg, 1.93 mmol) and DMAP (50 mg, 0.41 mmol) were added to the rhod-B hydrazone (RHH) (900 mg, 1.91 mmol) in dry methylene chloride (30 mL). The mixture was dissolved in dry methylene chloride and chilled at 0 °C followed by the addition of DCC (800 mg, 3.88 mmol). The reaction mixture was stirred under nitrogen atmosphere at 0 °C for 15 min and then at room temperature for 10–12 h. The precipitated urea was removed by filtration, and the filtrate was concentrated in high vacuum to give an oily residue. This residue was purified by column chromatography using silica gel (100–200 mesh) and 15% ethyl acetate in petroleum ether as eluent to afford the target compound RHHP as a white solid: yield, 700 mg, 54%; mp 95–100 °C.

**$^1\text{H NMR}$**  ( $\text{CDCl}_3$ , 300 MHz).  $\delta$  (ppm): 8.216 (s, 1H), 7.810 (t, 1H,  $J = 6 \text{ Hz}$ ), 7.440 (q, 1H,  $J = 9.6$ ), 7.084 (t, 1H,  $J = 7.3 \text{ Hz}$ ), 6.485 (m, 2H), 6.336 (s, 1H), 6.28 (t, 2H,  $J = 2.8 \text{ Hz}$ ), 6.218 (t, 2H,  $J = 12 \text{ Hz}$ ), 4.950 (s, 1H), 3.253 (t, 8H,  $J = 5.1 \text{ Hz}$ ), 2.196 (t, 8H,  $J = 5.1 \text{ Hz}$ ), 2.119 (t, 2H,  $J = 6 \text{ Hz}$ ), 1.103 (t, 12H,  $J = 3.3 \text{ Hz}$ ).

**$^{13}\text{C NMR}$**  ( $\text{CDCl}_3$ , 75 MHz).  $\delta$  (ppm): 179.25, 178.57, 170.78, 164.86, 153.85, 153.25, 150.75, 148.92, 143.72, 134.07, 133.08, 129.60, 128.29, 124.65, 124.13, 123.27, 108.12, 107.76, 106.46, 104.21, 104.12, 97.36, 66.58, 55.68, 54.39, 50.47, 44.22, 39.39, 32.45, 31.98, 31.26, 30.21, 29.44, 28.86, 25.79, 25.36, 25.27, 24.78.

**HRMS (ESI-TOF)**  $m/z$ . M+ calcd for  $\text{C}_{38}\text{H}_{44}\text{N}_6\text{O}_6$ , 680.3322; found, 679.3821(M – H)<sup>+</sup>.

## ASSOCIATED CONTENT

### S Supporting Information

Detailed characterization of the compound sensor RHHP along with the isolated products from the reaction RHHP +  $\text{OCl}^-$ , additional spectroscopic details, spectra, and crystallographic analysis. This material is available free of charge via the Internet at <http://pubs.acs.org>.

## AUTHOR INFORMATION

### Corresponding Author

\*Fax: +91 33 2668 2916. Phone: +91 33 2668 2961-3. E-mail: spgoswamical@yahoo.com.

### Notes

The authors declare no competing financial interest.

## ACKNOWLEDGMENTS

The authors thank the DST and CSIR (Government of India) for financial support. A.K.D., A.M., and A.K.M. acknowledge the CSIR for providing fellowships. The authors extend their sincere appreciation to the Deanship of Scientific Research at King Saud University for its funding of this research through the Research Group Project no. RGP-VPP-321.

## REFERENCES

- (1) Aokl, T.; Munemorl, M. *Anal. Chem.* 1983, 55, 209.
- (2) (a) Sun, Z.; Liu, F.; Chen, Y.; Yang, D. *Org. Lett.* 2008, 10, 2171. (b) Goswami, S.; Manna, A.; Paul, S.; Quah, C. K.; Fun, H.-K. *Chem. Commun.* 2013, 49, 11656. (c) Goswami, S.; Das, A. K.; Sen, D.; Aich, K.; Fun, H.-K.; Quah, C. K. *Tetrahedron Lett.* 2012, 53, 4819. (d) Goswami, S.; Das, A. K.; Aich, K.; Manna, A. *Tetrahedron Lett.* 2013, 54, 4215. (e) Goswami, S.; Das, A. K.; Manna, A.; Maity, A. K.; Fun, H.-K.; Quah, C. K.; Saha, P. *Tetrahedron Lett.* 2014, 55, 2633. (f) Goswami, S.; Paul, S.; Manna, A. *Dalton Trans.* 2013, 42, 10097.

- (3) (a) Gomes, A.; Fernandes, E.; Lima, J. L. F. C. *J. Biochem. Biophys. Methods* **2005**, *65*, 45. (b) Oushiki, D.; Kojima, H.; Terai, T.; Arita, M.; Hanaoka, M.; Hanaoka, K.; Urano, Y.; Nagano, T. *J. Am. Chem. Soc.* **2010**, *132*, 2795. (c) Li, X. H.; Zhang, G. X.; Ma, H. M.; Zhang, D. Q.; Li, J.; Zhu, D. B. *J. Am. Chem. Soc.* **2004**, *126*, 11543. (d) Bizyukin, A. V.; Korkina, L. G.; Velichkovskii, B. T. *Bull. Exp. Biol. Med.* **1995**, *119*, 347.
- (4) (a) Harrison, J. E.; Schultz, J. *J. Biol. Chem.* **1976**, *251*, 1371. (b) Panizzi, P.; Nahrendorf, M.; Wildgruber, M.; Waterman, P.; Figueiredo, J. L.; Aikawa, E.; McCarthy, J.; Weissleder, R.; Hilderbrand, S. A. *J. Am. Chem. Soc.* **2009**, *131*, 15739.
- (5) (a) Kettle, A. J.; Winterbourn, C. C. *Redox Rep.* **1997**, *3*, 3. (b) Pattison, D. I.; Davies, M. *J. Chem. Res. Toxicol.* **2001**, *14*, 1453. (c) O'Brien, P. *J. Chem.—Biol. Interact.* **2000**, *129*, 113.
- (6) (a) Podrez, E. A.; Abu-Soud, H. M.; Hazen, S. L. *Free Radical Biol. Med.* **2000**, *28*, 1717. (b) Pattison, D. I.; Davies, M. *J. Biochemistry* **2006**, *45*, 8152.
- (7) Berry, D.; Xi, C.; Raskin, L. *Curr. Opin. Biotechnol.* **2006**, *17*, 297.
- (8) Vital, M.; Stucki, D.; Egli, T.; Hammes, F. *Appl. Environ. Microbiol.* **2010**, *76*, 6477.
- (9) Williams, M. M.; Domingo, J. W. S.; Meckes, M. C.; Kelty, C. A.; Rochon, H. S. *J. Appl. Microbiol.* **2004**, *96*, 954.
- (10) Pinto, A. J.; Xi, C.; Raskin, L. *Environ. Sci. Technol.* **2012**, *46*, 8851.
- (11) (a) Kenmoku, S.; Urano, Y.; Kojima, H.; Nagano, T. *J. Am. Chem. Soc.* **2007**, *129*, 7313. (b) Koide, Y.; Urano, Y.; Hanaoka, K.; Terai, T.; Nagano, T. *J. Am. Chem. Soc.* **2011**, *133*, 5680.
- (12) Chen, X.; Wang, X.; Wang, S.; Shi, W.; Wang, K.; Ma, H. *Chem.—Eur. J.* **2008**, *14*, 4719.
- (13) Yang, Y. K.; Cho, H. J.; Lee, J.; Shin, I.; Tae, J. *Org. Lett.* **2009**, *11*, 859.
- (14) (a) Cheng, X.; Jia, H.; Long, T.; Feng, J.; Qin, J.; Li, Z. *Chem. Commun.* **2011**, *47*, 11978. (b) Shi, J.; Li, Q.; Zhang, X.; Peng, M.; Qin, J.; Li, Z. *Sens. Actuators, B* **2010**, *145*, 583. (c) Lin, W.; Long, L.; Chen, B.; Tan, W. *Chem.—Eur. J.* **2009**, *15*, 2305.
- (15) Panizzi, P.; Nahrendorf, M.; Wildgruber, M.; Waterman, P.; Figueiredo, J. L.; Aikawa, E. *J. Am. Chem. Soc.* **2009**, *131*, 15739.
- (16) (a) Lou, X.; Zhang, Y.; Qin, J.; Li, Zhen *Sens. Actuators, B* **2012**, *161*, 229. (b) Wang, Q.; Tan, C.; Cai, W. *Analyst* **2012**, *137*, 1872.
- (17) Long, L.; Zhang, D.; Li, X.; Zhang, J.; Zhang, Chi.; Zhou, L. *Anal. Chim. Acta* **2013**, *775*, 100.
- (18) (a) Domaille, D. W.; Que, E. L.; Chang, C. *J. Nat. Chem. Biol.* **2008**, *4*, 168. (b) Ueno, T.; Nagano, T. *Nat. Methods* **2011**, *8*, 642. (c) Du, J.; Hu, M.; Fan, J.; Peng, X. *Chem. Soc. Rev.* **2012**, *41*, 4511. (d) Vendrell, M.; Zhai, D.; Er, J. C.; Chang, Y. T. *Chem. Rev.* **2012**, *112*, 4391. (e) Goswami, S.; Sen, D.; Das, N. K.; Fun, H.-K.; Quah, C. K. *Chem. Commun.* **2011**, *47*, 9101. (f) Kumar, M.; Kumar, N.; Bhalla, V.; Singh, H.; Sharma, P. R.; Kaur, T. *Org. Lett.* **2011**, *13*, 1422. (g) Goswami, S.; Das, A. K.; Aich, K.; Manna, A.; Maity, S.; Khanra, K.; Bhattacharyya, N. *Analyst* **2013**, *138*, 4593. (h) Goswami, S.; Das, A. K.; Maity, S. *Dalton Trans.* **2013**, *42*, 16259. (i) Goswami, S.; Manna, A.; Maity, A. K.; Paul, S.; Das, A. K.; Das, M. K.; Saha, P.; Quah, C. K.; Fun, H.-K. *Dalton Trans.* **2013**, *42*, 12844. (j) Goswami, S.; Das, A. K.; Maity, A. K.; Manna, A.; Aich, K.; Maity, S.; Saha, P.; Mandal, T. K. *Dalton Trans.* **2014**, *43*, 231.
- (19) Yang, X. F.; Guo, X. Q.; Zhao, Y. B. *Talanta* **2002**, *57*, 883.
- (20) (a) He, G.; Zhang, X.; He, C.; Zhao, X.; Duan, C. *Tetrahedron* **2010**, *66*, 9762. (b) Yuan, L.; Lin, W.; Chen, B.; Xie, Y. *Org. Lett.* **2012**, *14*, 432. (c) Kumar, M.; Kumar, N.; Bhalla, V.; Sharma, P. R.; Kaur, T. *Org. Lett.* **2012**, *14*, 406. (d) Zhang, J. F.; Zhou, Y.; Yoon, J.; Kim, Y.; Kim, S. J.; Kim, J. S. *Org. Lett.* **2010**, *12*, 3852.